

## Matching Fingers in the Four Rod RFQ

P. Junior, M. Malouschek, J. Dehen

Institut für Angewandte Physik

Robert-Mayer-Straße 2-4, D-6000 Frankfurt am Main, Fed. Rep. of Germany

### Abstract

Matching the DC beam to the four rod RFQ is accomplished by straight or bent fingers. The paper reports behavior of several configurations with respect to radial mismatch factors and outcoming energy spread.

### 1. POTENTIALFUNCTION

Following suggestions as reported in [1],[2] the discussion is based on the potentialfunction

$$\begin{aligned} \phi(r, z, \vartheta, t) &= \frac{AV}{2} \cos \omega t [\cos 2\vartheta F_1(r, z) + \cos 6\vartheta F_2(r, z)] \\ F_1(r, z) &= \sum_{j=1}^{i_{\max}} C_j I_2(ikr) \cos(ikz) \\ F_2(r, z) &= \sum_{j=1}^{i_{\max}} D_j I_6(ikr) \cos(ikz) \end{aligned} \quad (1)$$

$i = 2j - 1$  here and in following equations

Cylindric coordinates  $r, \vartheta, z$ , particle velocity  $v$ ,  $\beta = v/c$ , vane voltage  $V$ , rf of RFQ  $f$ ,  $\omega = 2\pi f$ , mean aperture  $R$ .

Fig. 1 illustrates the corresponding periodic sequence of the electrodes, where the section from  $z = -L$  to  $z = 0$  is investigated. This distance amounts to  $(N+1)\beta\lambda/2$  cells defining the matcher as well as its wave number  $k = \pi/2L$ .

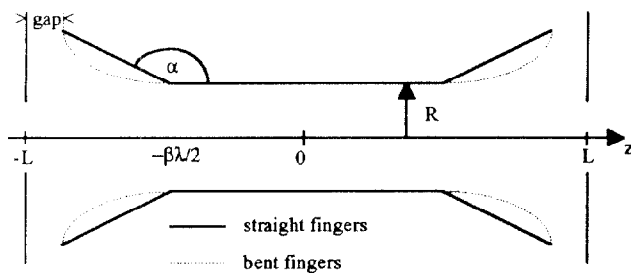


Fig. 1 Periodic electrode sequence

A stands for the regular transition of the potential (1) to the one, which starts with plain electrodes from  $z = 0$  on.

$$A^{-1} = \sum_i^{i_{\max}} (C_j I_2(jkr) + D_j I_6(jkr)) \quad (2)$$

The Fourier coefficients  $C_j$  characterize the slope of the fieldgradients

$$E'(z) = \frac{V}{R^2} \frac{\sum_j^2 C_j \cos(jkz)}{\sum_j^2 C_j} \quad (3)$$

For bent electrodes they are chosen such, that the slopes have the form of trapezoid. This is shown in fig. 2, where the choice with integer  $M, j = 2i - 1, i = 1$  to  $i_{\max} = 5$  is

$$C_j = \frac{1}{j!} (-1)^{i+1} \sin\left(\frac{\pi}{8} j M\right) \quad (4)$$

In case of a matcher with straight fingers (angle  $\alpha$  in fig. 1) the  $C_i$  are determined by way of a least square fit of the potential equ. (1) (with all  $D_j = 0$ ) to the electrode potential  $V/2$  with an aperture function  $s(z)$  according to

$$\frac{\delta}{\delta C_j} \int_0^{-L} \left[ \phi(s(z), z, \vartheta = 0, t = 0) - \frac{U}{2} \right]^2 dz = 0 \quad (5a)$$

On the electrodes  $-L+g \leq z \leq 0, U = AV$ , in the gap from  $-L$  to  $-L+g$  the potential slope along the dotted line was calculated with [3]. If we regard a four rod configuration, the rod radius should obviously be kept constant, and may for an example agree with the free aperture  $R$ . Corresponding  $D_j$ 's can again be evaluated with a least square fit. In this case the set of inhomogeneous linear equations with degree  $i_{\max}$  for the unknown  $D_j$  is derived from

$$\frac{\delta}{\delta D_j} \int_0^{-L} \left[ R_2(z) \frac{\delta \phi}{\delta r} - \frac{\delta^2 \phi}{\delta \vartheta^2} \right]_{s(z), z, \vartheta=0, t=0} = 0 \quad (5b)$$

$$R_2(z) = -s(z) \left[ \frac{s(z)}{R} + 1 \right]$$

Of course the interpolation of the potential within the gap is accomplished in the same way as in (5a), given  $C_j$ 's included. For bent electrodes  $i_{\max} = 5$  suffices, straight fingers, however, require  $i_{\max} \geq 10$ . Table 1 exemplarily shows coefficients of an optimized matcher design and fig. 2 and 3 give examples of fieldgradient slopes and corresponding matcher configurations.

Table 1 Coefficients for  $k = \pi/2\beta\lambda, M = 2$

|                      |                      |
|----------------------|----------------------|
| $C(1) = 0.7071+000$  | $D(1) = 0.3039+001$  |
| $C(3) = -0.8730-002$ | $D(3) = -0.8829-002$ |
| $C(5) = -0.1131-002$ | $D(5) = 0.3638-003$  |
| $C(7) = 0.2945-003$  | $D(7) = -0.3035-004$ |
| $C(9) = 0.1078-003$  | $D(9) = 0.3367-005$  |

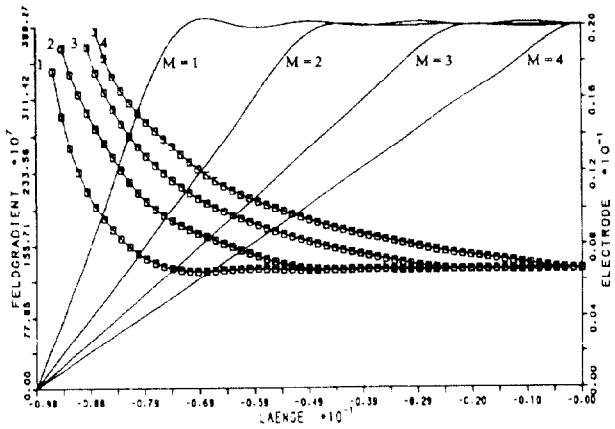


Fig. 2 Scheme of bent fingers and corresponding fieldgradients, N = 4

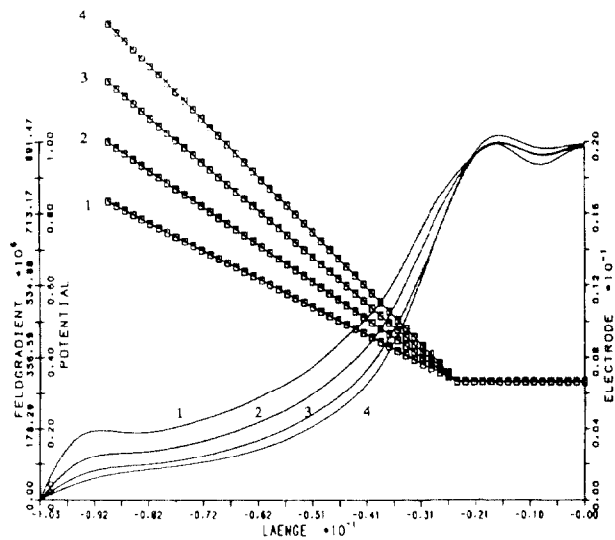


Fig. 3 Scheme of straight fingers and corresponding fieldgradients, N = 3, gap =  $\beta\lambda/4$

2. MOTION

Transverse particle motion follows the equation

$$\frac{d^2r}{dt^2} = \frac{eAVk}{2m} \cos(\omega t + \varphi) [\cos 2\vartheta G_1(r, z) + \cos 6\vartheta G_2(r, z)]$$

$$G_1(r, z) = \sum_{j=1}^3 jC_j \left[ I_1(jkr) - \frac{2}{jkr} I_2(jkr) \right] \cos(jkz)$$

$$G_2(r, z) = \sum_{j=1}^3 jD_j \left[ I_5(jkr) - \frac{6}{jkr} I_6(jkr) \right] \cos(jkz) \tag{6}$$

while the longitudinal equation is

$$\frac{d^2u}{dt^2} = \frac{eAVk}{2m} \cos(\omega t + \varphi) [\cos 2\vartheta H_1(r, z) + \cos 6\vartheta H_2(r, z)]$$

$$H_1(r, z) = \sum_{i=1}^4 jC_i I_2(jkr) \sin jkz$$

$$H_2(r, z) = \sum_{i=1}^4 jD_i I_6(jkr) \sin jkz \tag{7}$$

u means the longitudinal deviation  $u = z - vt + L$  of the particle with respect to the unpertubated particle on the axis  $r = 0, u(t) = 0$ . At  $z = 0$  the acceptance of the RFQ rotates with variable phase  $\varphi$ , in which dc particles may enter. Fig. 4 illustrates the small remaining area of about 38% with respect to the acceptance of any one of the rotating ellipses. So a useful matcher should increase this area by a considerable amount, and fig. 5 shows a gain up to 90%, which may be achieved with the proper matcher. For these determinations transport of particles which coincide with corresponding acceptance ellipses using equ. (6) and (7) was numerically carried on from  $z = 0$  backwards to  $z = -L$  for many phases in  $0 \leq \varphi \leq 2\pi$ .

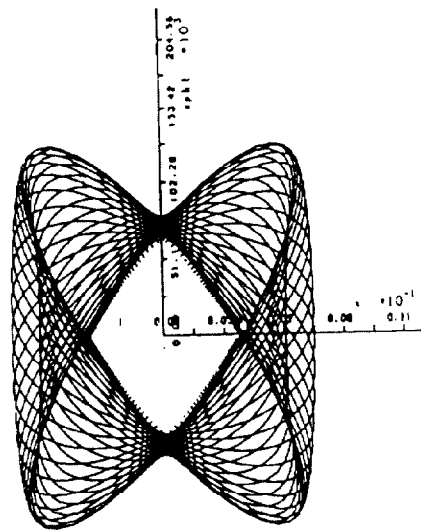


Fig. 4 Voluting acceptance at  $z = 0$

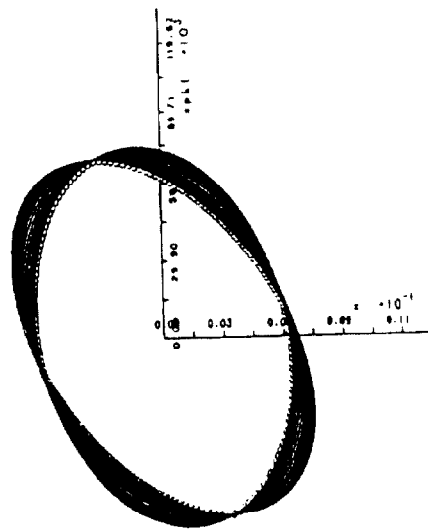


Fig. 5 Voluting acceptance at  $z = -L$

For the calculations with beam currents  $\neq 0$  equ. (6) and (7) were supplemented by proper KV space charge terms [4]. Tables 2 and 3 demonstrate variations of N and M acc. to equ.'s (4) and (8), table 4 comprehends the optimum configurations.

Table 2

f = 16.9 MHz, E = 10 keV, V = 3.7 kV, I = 6.5 mA,  $\sigma_0 = 90^\circ$ , He<sup>+</sup>, R = 5.0 mm, bent fingers left, straight fingers right

| n | m | area[%] |
|---|---|---------|---|---|---------|---|---|---------|---|---|---------|
| 1 | 1 | 22.89   | 5 | 1 | 39.27   | 1 | 1 | 48.36   | 5 | 1 | 64.80   |
| 1 | 2 | 27.10   | 5 | 2 | 74.05   | 1 | 2 | 35.87   | 5 | 2 | 59.73   |
| 1 | 3 | 28.33   | 5 | 3 | 37.15   | 1 | 3 | 41.91   | 5 | 3 | 66.45   |
| 1 | 4 | 34.86   | 5 | 4 | 45.91   | 1 | 4 | 64.22   | 5 | 4 | 78.06   |
| 2 | 1 | 17.85   | 6 | 1 | 27.01   | 2 | 1 | 54.86   | 6 | 1 | 77.15   |
| 2 | 2 | 26.07   | 6 | 2 | 44.40   | 2 | 2 | 62.64   | 6 | 2 | 64.30   |
| 2 | 3 | 40.36   | 6 | 3 | 38.65   | 2 | 3 | 65.98   | 6 | 3 | 60.75   |
| 2 | 4 | 60.91   | 6 | 4 | 55.89   | 2 | 4 | 78.17   | 6 | 4 | 69.05   |
| 3 | 1 | 18.43   | 7 | 1 | 34.62   | 3 | 1 | 59.36   | 7 | 1 | 88.25   |
| 3 | 2 | 28.75   | 7 | 2 | 53.66   | 3 | 2 | 64.74   | 7 | 2 | 78.53   |
| 3 | 3 | 45.77   | 7 | 3 | 65.51   | 3 | 3 | 67.50   | 7 | 3 | 65.10   |
| 3 | 4 | 57.27   | 7 | 4 | 42.86   | 3 | 4 | 66.67   | 7 | 4 | 59.09   |
| 4 | 1 | 34.59   | 8 | 1 | 68.08   | 4 | 1 | 58.19   | 8 | 1 | 72.71   |
| 4 | 2 | 43.36   | 8 | 2 | 46.62   | 4 | 2 | 62.43   | 8 | 2 | 88.46   |
| 4 | 3 | 65.24   | 8 | 3 | 33.38   | 4 | 3 | 70.97   | 8 | 3 | 80.01   |
| 4 | 4 | 55.48   | 8 | 4 | 48.70   | 4 | 4 | 75.95   | 8 | 4 | 66.77   |

Table 3

f = 27 MHz, E = 300 keV, V = 180 kV, I = 20 mA,  $\sigma_0 = 25^\circ$ , Xe<sup>1+</sup>, R = 6.8 mm, bent fingers left, straight fingers right

| n | m | area[%] |
|---|---|---------|---|---|---------|---|---|---------|---|---|---------|
| 1 | 1 | 38.48   | 5 | 1 | 50.56   | 1 | 1 | 80.11   | 5 | 1 | 89.16   |
| 1 | 2 | 47.53   | 5 | 2 | 76.71   | 1 | 2 | 80.51   | 5 | 2 | 94.44   |
| 1 | 3 | 53.86   | 5 | 3 | 68.47   | 1 | 3 | 83.82   | 5 | 3 | 97.45   |
| 1 | 4 | 61.68   | 5 | 4 | 75.44   | 1 | 4 | 88.10   | 5 | 4 | 99.03   |
| 2 | 1 | 34.20   | 6 | 1 | 76.63   | 2 | 1 | 89.27   | 6 | 1 | 83.66   |
| 2 | 2 | 41.99   | 6 | 2 | 85.81   | 2 | 2 | 91.13   | 6 | 2 | 89.60   |
| 2 | 3 | 58.34   | 6 | 3 | 85.01   | 2 | 3 | 92.62   | 6 | 3 | 94.05   |
| 2 | 4 | 77.50   | 6 | 4 | 75.18   | 2 | 4 | 93.18   | 6 | 4 | 97.20   |
| 3 | 1 | 46.08   | 7 | 1 | 53.97   | 3 | 1 | 91.04   | 7 | 1 | 78.83   |
| 3 | 2 | 64.71   | 7 | 2 | 71.48   | 3 | 2 | 94.34   | 7 | 2 | 84.01   |
| 3 | 3 | 72.81   | 7 | 3 | 72.87   | 3 | 3 | 95.78   | 7 | 3 | 78.56   |
| 3 | 4 | 85.96   | 7 | 4 | 68.81   | 3 | 4 | 96.66   | 7 | 4 | 92.33   |
| 4 | 1 | 48.11   | 8 | 1 | 86.61   | 4 | 1 | 91.96   | 8 | 1 | 74.69   |
| 4 | 2 | 87.98   | 8 | 2 | 85.77   | 4 | 2 | 95.58   | 8 | 2 | 78.45   |
| 4 | 3 | 67.19   | 8 | 3 | 85.37   | 4 | 3 | 97.46   | 8 | 3 | 82.75   |
| 4 | 4 | 80.16   | 8 | 4 | 85.86   | 4 | 4 | 98.63   | 8 | 4 | 86.47   |

In tables referring to straight fingers m is related to  $\alpha$  according to

$$\tan \alpha = - \frac{(\frac{M}{2} + 1) * R}{N * \frac{R\lambda}{2} - g} \tag{8}$$

Table 4

Normalized emittance  $\epsilon_n$  and energy spread  $\delta W/W$  for the optimised matcher configuration of table 2 and 3

| f [MHz] | form     | I [mA] | $\sigma_0$ [°] | n | m | $\epsilon_n$ [mmrad] | $\delta W/W$ [%] |
|---------|----------|--------|----------------|---|---|----------------------|------------------|
| 16.9    | bent     | 6.5    | 90             | 5 | 2 | 0.2                  | 0.12             |
| 16.9    | straight | 6.5    | 90             | 2 | 4 | 0.2                  | 0.08             |
| 16.9    | straight | 6.5    | 90             | 8 | 2 | 0.2                  | 0.013            |
| 27.0    | bent     | 20.0   | 25             | 4 | 2 | 0.3                  | 0.31             |
| 27.0    | straight | 20.0   | 25             | 5 | 4 | 0.3                  | 0.19             |

### 3. CONCLUSIONS

Table 4 also lists energy spreads resulting from the solutions of equ. (6) and (7). In these simulations the overlap area was transported from  $z = -L$  to  $z = 0$ . It turns out that

- 1.) energy spread is considerable
- 2.) the  $D_j$ 's resp. the rod radius only play a minor role
- 3.) energy spread is almost equipartioned over the whole phase area
- 4.) energy spread is proportional to the illumination of the overlap by the dc beam emittance, so when both phase space coordinates are halved, energy spread is halved too
- 5.) bent and straight fingers behave slightly different
- 6.) satisfying overlaps turn out better at smaller  $\sigma_0$
- 7.) the last example in table 4 indicates, that in a long matcher energy spread is compensated

As a consequence considerable small and concentric beam emittance is demanded.

### 4. REFERENCES

- [1] K. R. Crandall, Proc. 1984 Lin Acc. Conf, GSI 84- 11, p. 109
- [2] P. Junior et al., Proc. 2nd EPAC, Nice 1990
- [3] P. Spätke, S. Wipf, KOBRA 3, GSI Report 89-09
- [4] I. M. Kapchinskij, V. V. Vladimirsij. Proc. Int. Conf. on High Energy Accelerators, Geneva 1959, p. 274

### Acknowledgements

The authors are indebted to the HRZ of the University of Frankfurt, the RFQ research program is sponsored by the BMFT.